Journal of Animal Ecology

British Ecological Society

Journal of Animal Ecology 2015, **84,** 590–603 doi: 10.1111/1365-2656.12346

Ocean sunfish rewarm at the surface after deep excursions to forage for siphonophores

Itsumi Nakamura*, Yusuke Goto and Katsufumi Sato

Atmosphere and Ocean Research Institute, The University of Tokyo, 5-1-5 Kashiwanoha, Kashiwa, Chiba 277-8564, Japan

Summary

1. Ocean sunfish (*Mola mola*) were believed to be inactive jellyfish feeders because they are often observed lying motionless at the sea surface. Recent tracking studies revealed that they are actually deep divers, but there has been no evidence of foraging in deep water. Furthermore, the surfacing behaviour of ocean sunfish was thought to be related to behavioural thermoregulation, but there was no record of sunfish body temperature.

2. Evidence of ocean sunfish feeding in deep water was obtained using a combination of an animal-borne accelerometer and camera with a light source. Siphonophores were the most abundant prey items captured by ocean sunfish and were typically located at a depth of 50–200 m where the water temperature was < 12 °C. Ocean sunfish were diurnally active, made frequently deep excursions and foraged mainly at 100–200 m depths during the day.

3. Ocean sunfish body temperatures were measured under natural conditions. The body temperatures decreased during deep excursions and recovered during subsequent surfacing periods. Heat-budget models indicated that the whole-body heat-transfer coefficient between sunfish and the surrounding water during warming was 3–7 times greater than that during cooling. These results suggest that the main function of surfacing is the recovery of body temperature, and the fish might be able to increase heat gain from the warm surface water by physiological regulation.

4. The thermal environment of ocean sunfish foraging depths was lower than their thermal preference (*c.* 16–17 °C). The behavioural and physiological thermoregulation enables the fish to increase foraging time in deep, cold water.

5. Feeding rate during deep excursions was not related to duration or depth of the deep excursions. Cycles of deep foraging and surface warming were explained by a foraging strategy, to maximize foraging time with maintaining body temperature by vertical temperature environment.

Key-words: animal-borne camera, body temperature, foraging, ocean sunfish, siphonophore, thermoregulation

Introduction

The pelagic zone is the largest area of the marine ecosystem, and predators are some of the most widely roaming and deepest diving species. Some pelagic predators dive into deep water to utilize food sources distributed in the mesopelagic zone (e.g. Aoki *et al.* 2012; Naito *et al.* 2013). Pelagic predatory fishes such as swordfish (*Xiphias gladius*) and blue sharks (*Prionace glauca*) mainly swim within the mixed layer but may approach greater depths (sometimes exceeded 1000 m) below the thermocline to forage (Carey & Robison 1981; Carey & Scharold 1990; Queiroz *et al.* 2012). Planktivores such as whale sharks (*Rhincodon typus*) and devil rays (*Mobula tarapacana*) also approach depths of over 1000 m in order to utilize deep water food sources (Brunnschweiler *et al.* 2009; Thorrold *et al.* 2014). These facts suggest that biomass of deep-sea ecosystems is sufficiently abundant to supply food to various pelagic predators that consume various types of prey. Jellyfishes such as medusae and siphonophores compose a large biomass in deep-sea ecosystems (Angel & Baker 1982), but there is little information regarding the predators of these jellyfishes.

The world's heaviest teleost, the ocean sunfish (*Mola mola* Linnaeus), is a known jellyfish feeder (Pope *et al.*

*Correspondence author. E-mail: itsumi@aori.u-tokyo.ac.jp

2010). Recent behavioural studies using accelerometers revealed that the fish are active swimmers (Watanabe & Sato 2008; Houghton *et al.* 2009), and tracking studies have discovered that ocean sunfish approach depths of up to 800 m (Sims *et al.* 2009a,b; Dewar *et al.* 2010; Potter & Howell 2011). These deep excursions were thought to be associated with foraging, but no empirical evidence about what they consume in deep water exists.

The name 'sunfish' refers to the animal's habit of lying motionless at the sea surface, a behaviour that resembles 'basking'. Hypotheses concerning the purpose of surfacing include sleeping, the elimination of external parasites by seabirds (Abe *et al.* 2012) and rewarming after excursions to deep, cold water (Cartamil & Lowe 2004). Sunfish remain at the surface after every deep excursion (Nakamura & Sato 2014), so it is difficult to determine whether the main function of this behaviour is parasite elimination. The surfacing behaviour might be behavioural thermoregulation (Cartamil & Lowe 2004); however, no empirical study has tested the thermal regulation hypothesis.

In this study, we used an animal-borne behavioural recorder (with an internal body temperature probe) and a camera with a light source to record the feeding events of ocean sunfish in deep water and to examine the thermal regulation hypothesis of surfacing behaviour by continuous measurement of body temperature under natural conditions.

Materials and methods

FIELD EXPERIMENTS

Fieldwork was conducted in July 2012 and July 2013 around Funakoshi Bay, Iwate, Japan (39°22′N, 141°58′E), where ocean sunfish are caught by set-nets managed by local fishermen during summer, and they are locally consumed as food. To collect behavioural data of free-ranging ocean sunfish, two different data loggers were used. This first option was an accelerometer data logger (W380-PD3GT; Little Leonardo, Tokyo, Japan; 21 mm in diameter, 116 mm in length and 60 g in air), which recorded tri-axial acceleration at 16 Hz and swimming speed, depth and temperature at 1 Hz. The second option was an accelerometer–magnetometer data logger (W1000-3MPD3GT; Little Leonardo; 26 mm in diameter, 166 mm in length and 132 g in air), which recorded tri-axial magnetism at 1 Hz in addition to the parameters of the W380-PD3GT accelerometer. To visually record sunfish feeding events, a digital video camera (DVL400; Little Leonardo; 22 mm in diameter, 80 mm in length and 40 g in air) or a digital still camera (DSL400-VDTII; Little Leonardo; 22 mm in diameter, 134 mm in length and 82 g in air) with an LED flashlight (LIT400-4LED; Little Leonardo; 22 mm in diameter, 124 mm in length and 98 g in air) were used. The video camera can record 720-pixel footage for a total of 70 min, and it was configured to start recording 2 days after release at a 10-min recording and 80-min resting cycle. The still camera can record an average of 9000 images depending on the image data size, and it was configured to record every 30 s in 2012 and every 4 s at depths deeper than 50 m in 2013. The LED flashlight flashed in synchronization with still image recordings. To measure body temperature, a depth temperature recorder (LAT1810ST; Lotek Wireless Inc., Newmarket, ON, Canada; 11 mm in diameter, 35 mm in length and 5 g in air with a 150-mm stalk temperature sensor), which recorded depth, ambient water temperature and body temperature at 1 Hz, was used. These devices were combined on a single-unit foam buoy with a retrieval system consisting of a time-release mechanism (RT-4; Little Leonardo; 16 mm diameter, 25 mm length and 16 g in air), a VHF transmitter (MM130B; Advanced Telemetry Systems, Isanti, MN, USA; 16 mm diameter, 60 mm length and 20 g in air) and a satellite transmitter (SPOT5; Wildlife Computers, Redmond, WA, USA; 10 mm, 20 mm, 80 mm length and 30 g in air) (Fig. 1). The packages were 320–710 g in air depending on the combination of devices.

Ocean sunfish were caught by three set-nets placed in Funakoshi Bay, which are managed by the Funakoshi Bay Fisheries Cooperative. The sunfish were brought onto the deck of the fishing vessel, measured [total length (TL) in cm] and equipped with instrument packages via metal cable ties threaded through a small hole pierced in back of the fish, anterior to their dorsal fin, that was secured around the package float (Watanabe & Sato 2008) (Fig. 1). In 2013 experiment, another vertical hole (<3 mm in diameter) was pierced and the stalk sensor of the depth temperature recorder was inserted; thus, the muscle temperature at a

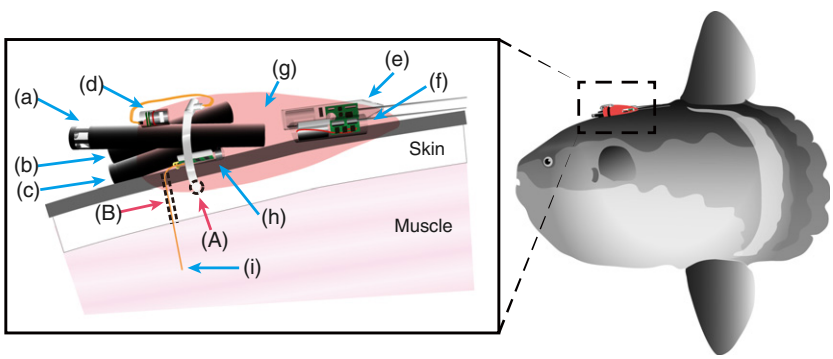

Fig. 1. Schematic diagram of accelerometer package and attachment method. Blue arrows indicate devices contained in the package: (a) an accelerometer–magnetometer data logger, (b) a digital still camera, (c) a LED flashlight, (d) a time-release mechanism, (e) a satellite transmitter, (f) a VHF transmitter, (g) a single-unit foam buoy, (h) a depth temperature recorder with the 15-cm stalk sensor (i). The instrument packages were equipped via metal cable ties threaded through a small hole (A) pierced in the back of the fish. Another vertical hole (B) was pierced, and the stalk sensor was inserted into the muscle.

depth of 15 cm from the body surface was measured (Fig. 1). Four sunfish (TL 125, 136, 148 and 200 cm) were released on 17–18 July 2012, and three sunfish (TL 105, 125 and 191 cm) were released on 12–13 July 2013, near the set-net where they were caught (Table 1). Instrument packages automatically detached from each sunfish after 4–6 days of deployment. The packages then floated to the surface, were located using the satellite and VHF transmitters and were retrieved by the 19-ton 'Koyo-maru' boat. These procedures were approved by the ethics committee at the University of Tokyo (Institutional Animal Case and Use Committee Protocol P12-14, P13-11).

ANALYSES OF BEHAVIOURAL AND VISUAL DATA

Igor Pro ver. 6.32A (WaveMetrics, Lake Oswego, OR, USA) was used to analyse behavioural data. Recorded accelerations included both low-frequency gravity components (caused by the changing pitch and roll angles of the body) and high-frequency specific components (caused by dynamic movements such as fin stroking). Specific and gravity components of acceleration were separated using a 0·01-Hz low-pass filter (contained within Igor Pro), which removes high-frequency waves to extract the gravity component. Then, the gravity component of acceleration was used to calculate the pitch of the sunfish from longitudinal acceleration and the roll from lateral and dorsoventral acceleration. The three-dimensional movement path of each sunfish equipped with accelerometer–magnetometers was reconstructed using a dead-reckoning method (Shiomi *et al*. 2010). Every 1 s step was calculated from the tri-axial magnetometer data (i.e. compass heading), data logger orientation, pitch and speed.

Whether possible prey objects or feeding events were seen in the images and footage recorded by the cameras were checked, and the prey items were identified to the lowest possible taxonomic level. After feeding events were determined from the visual data, the characteristics of these events were identified in the behavioural data. Because the cameras could not cover the entire deployment period, the feeding events were extracted from the full behavioural data, and when and how deep the events occurred were estimated.

ANALYSES OF BODY TEMPERATURE

For the body temperature analysis, changes in the whole-body heat-transfer coefficient k that is necessary to account for the observed rates of body warming and cooling were estimated using a function of heat exchange with the environment and internal heat production (Holland & Sibert 1994; Kitagawa *et al*. 2001). Heat loss (or gain) is proportional to the difference between the body temperature of the sunfish and the water in which it is swimming:

$$\frac{\mathrm{d}T_b(t)}{\mathrm{d}t} = k(T_a(t) - T_b(t)) + \dot{T}_0 + \varepsilon, \qquad \text{eqn 1}$$

where k is the whole-body heat-transfer coefficient (°C min^{-1} °C^{-1}), $T_a(t)$ is the ambient water temperature (°C) as a function of time t (min), $T_b(t)$ is the body temperature of sunfish (°C) as a function of time t, $\dot{T}_0$ is the rate of temperature change due to internal heat production (°C min^{-1}), and ε is white Gaussian noise. The response time-lag of body temperature behind the ambient water temperature was observed in the measured body temperature. Therefore, τ (min) was added as the response time-lag of body temperature:

$$\frac{\mathrm{d}T_b(t)}{\mathrm{d}t} = k(T_a(t-\tau) - T_b(t)) + \dot{T}_0 + \varepsilon. \qquad \text{eqn 2}$$

The following two conditions about k were assumed:

$$(a)\ k = \text{a constant value},$$

$$(b)\ k = \begin{cases} k_1; T_a(t-\tau) < T_b(t) \\ k_2; T_a(t-\tau) \geq T_b(t) \end{cases},$$

where k_1 and k_2 are two values for the heat-transfer coefficient. The parameters for each model were estimated using a maximum-likelihood method. Equation (2) was discretized in time using the Euler–Maruyama scheme (Kloeden & Platen 1999). The time evolution of T_b^t, the body temperature at the time point t, is written as follows:

$$T_b^{t+1} = T_b^t + \Delta t\{k(T_a^{t-\tau} - T_b^t) + \dot{T}_0\} + \sigma\eta^t\sqrt{\Delta t}, \qquad \text{eqn 3}$$

where Δt is a time interval between the adjoined time points at t and $t + 1$. In the following analysis, $\Delta t = 1$ (min) was used. $T_a^{t-\tau}$ is the ambient water temperature at a time point $t-\tau$, and σ is the noise intensity. The noise η^t is generated from a standard normal distribution. The estimated parameters are k, σ and τ. Given the time-series data $T_b = \{T_b^t\}(t = 1, \cdots, T)$ and

Table 1. Summary of deployed individuals

Fish ID	Total length (cm)	Release date	Estimated body mass (kg)	Duration (days)	Travel distance (km)	Calculated travel distance (km)	Data logger	Camera
MOLA1	136	17 July 2012	132	6	138	31	AM	SL
MOLA2	148	17 July 2012	169	6	160	31	AM	
MOLA3	200	17 July 2012	412	6	176	79	AM	SL
MOLA4	125	18 July 2012	103	5	126	52	AM	SL
MOLA5	105	12 July 2013	61	5	159	16	AM	SL[a]
MOLA6	125	13 July 2013	103	4	150		A	V
MOLA7	191	13 July 2013	360	4	192	82	AM	SL

Estimated body masses were calculated according to a length–mass relationship (Watanabe & Sato 2008). Travel distance indicates the straight distance between release and package pop-up locations. Calculated travel distance indicates the straight distance between the start and end of the horizontal movement path calculated by a dead-reckoning method. The data logger column indicates the use of either an accelerometer–magnetometer W1000-3MPD3GT (AM) or an accelerometer W380-PD3GT (A). The camera column indicates the use of a still camera DSL400-VDTII with LED light LIT400-4LED (SL) or a video camera DVL400 (V).
[a]Camera did not work.

$T_a = \{T_a^t\}(t = 1-\tau, \cdots, T-\tau)$, the conditional probability $P(T_b, T_a|k, \sigma, \tau) = \prod_{t=1}^{N} P(T_b^t|T_b^{t-1}, T_a^{t-\tau}, k, \sigma, \tau)$ and likelihood can be calculated with eqn (3).

R ver. 3.0.2 (R Core Team 2013) and the 'optim' function was used to maximize the likelihood by adjusting all parameters and calculating the Bayesian information criterion (BIC) of models (*a*) and (*b*). The model that showed the lower BIC was regarded as a parsimonious model.

To examine whether the heat-transfer coefficient changed under deceased conditions, the body temperature change of a dead sunfish (TL 32 cm) was recorded by placing the fish alternately in Styrofoam cartons containing 18 and 8 °C sea water. Body temperature and water temperature were measured using the LAT1810ST depth temperature recorder, and the data were subsequently analysed using the heat-budget model. Regarding the dead sunfish, the rate of temperature change due to internal heat production ($\dot{T}_0$) was assumed to be 0.

Results

ANALYSIS OF BEHAVIOURAL DATA

All instruments were retrieved, yielding a total of 33 days of behavioural data from seven sunfish, with a total of 47 676 still images from four individuals and 70 min of video footage from one individual. A total of 13 days of body temperature measurements were also obtained from three of the seven individuals. All sunfish migrated south (the farthest point was 192 km away from the release point; Table 1) during the 4–6 day deployment, where the sea surface temperature was 20–22 °C and the chlorophyll *a* concentration from remotely sensed data ranged 0·2–0·4 mg m^{-3} (Fig. 2). All sunfish showed typical day–night behaviour (the border between day and night was defined by civil dawn and dusk when the sun is 6 degrees below the horizon) and repetitively approached over 100 m from the surface during the day, but stayed at shallow depths (0–20 m) during the night (Fig. 3a,b). The ambient water temperature was 16–22 °C at the surface, and the fish experienced <10 °C at depths over 100 m (Fig. 3a,c). During the day, sunfish ranged over 200 m from the surface and spent about 40% of their time at the surface (0–5 m), and they spent >95% of their time at shallow depths (0–20 m) during the night (Fig. 3b). Both during the day and the night, the peak ambient water temperature was 16–18 °C, but the range was wider during the day than that during the night (Fig. 3c). During the day, sunfish were active (swimming speed >0·2 m s^{-1}) during deep excursions, but inactive at the surface (swimming speed 0–0·2 m s^{-1} for >60% of time while at the surface) (Fig. 3d). Sunfish kept a relatively vertical position (roll was between −60° and 60°) during deep excursions, and the roll was distributed with relatively uniformity (from a vertical to lateral position) while at the surface (Fig. 3e). During the night, sunfish were inactive (swimming speed 0–0·2 m s^{-1} for >70% of time) in a lateral position (roll was >60° or <−60°) (Fig. 3d,e).

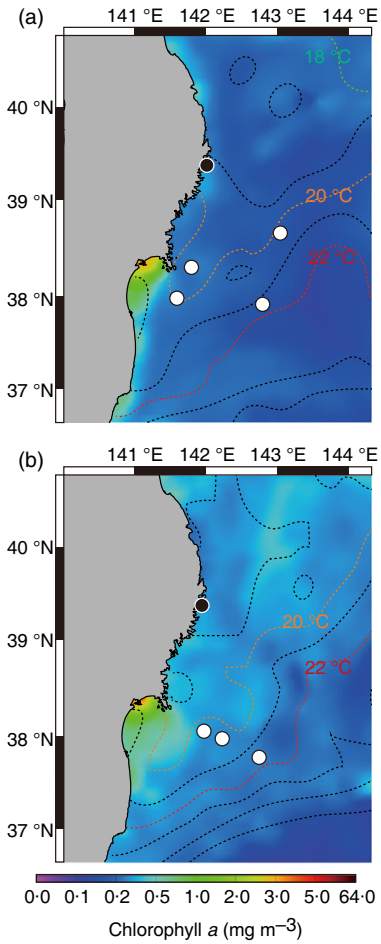

Fig. 2. Maps of release points (black circles) and package pop-up locations (open circles) in (a) 2012 and (b) 2013. Dotted lines indicate isothermal lines of sea surface temperatures on the package pop-up date (Japan Meteorological Agency 2013). Contour colours indicate monthly chlorophyll *a* concentration in July (SEATURTLE.ORG Maptool 2002).

FORAGING BEHAVIOUR

MOLA6, on which the digital video camera was deployed, encountered a blue shark (*P. glauca*) at a depth of 2 m (Fig. 4a); however, it was difficult to see anything in the footage because of the lack of light in deep water. On the other hand, images of putative prey items were obtained from all the sunfish deployed with digital still cameras with LED lights, except MOLA5 because of recording issues. Prey items were distinguished from a total of 323 still images (0·68% of 47 676 images) recorded by four sunfish (Table 2). The images taken in water shallower than 40 m during the day were white because the camera sensitivity was fixed at high for deep, dark water. The prey items belonged to at least three genera of siphonophores (*Praya* sp., *Nanomia* sp. and *Apolemia* sp.), scyphozoa (*Cyanea capillata* and *Chrysaora pacifica*) and ctenophores (*Beroe* sp. and Cydippida) (see examples, Fig. 4b–f). Siphonophores were the most observed of all individuals (Table 2). All

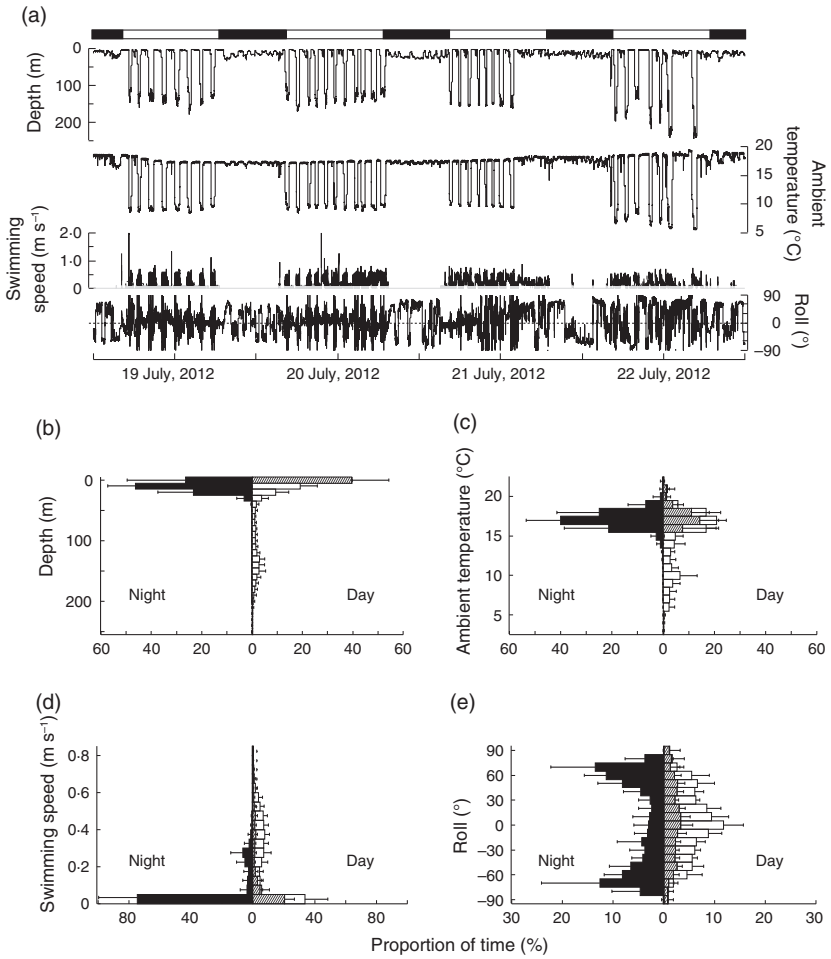

Fig. 3. (a) An example of time-series depth, ambient temperature, swimming speed and roll from MOLA1. The bar above the graph indicates night (black) and day (white). The swimming speed under the stall speed of the speed sensors (0·1–0·2 m s^{-1}) is shown in grey. Frequency histograms of (b) depth, (c) ambient temperature, (d) swimming speed and (e) roll during the day (white and shaded bars indicate deep excursions and remaining at the surface (depth < 5 m), respectively) and night (black bars). The histograms show the mean value of all individuals, and error bars indicate the standard deviation among individuals.

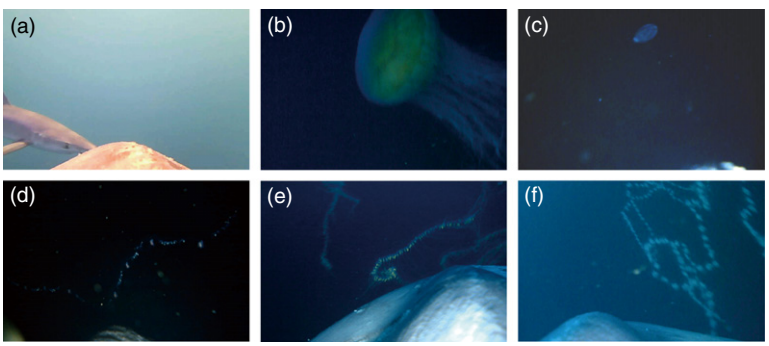

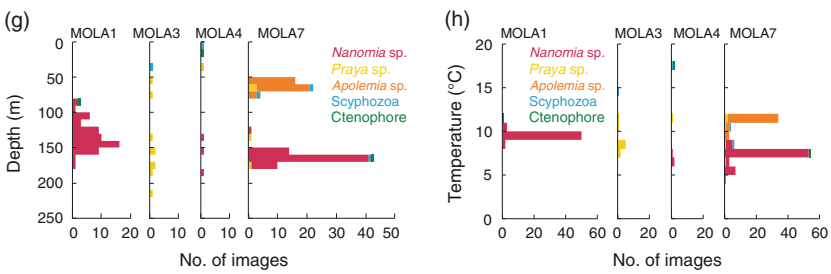

Fig. 4. Images taken by an animal-borne camera (a–f) as well as the depth (g) and temperature (h) distribution of each prey item. Images show (a) a blue shark crossing in front of the sunfish, (b) a lion's mane jellyfish (*Cyanea capillata*), (c) a ctenophore (*Beroe* sp.), (d) a siphonophore chain (*Nanomia* sp.), (e) a siphonophore chain (*Praya* sp.) and (f) a siphonophore chain (*Apolemia* sp.).

images with prey items except two (*C. pacifica* and *Beroe* sp.) were recorded during the day. The peak prey occurrence depth was 50–200 m, where the ambient water temperature ranged 5–12 °C (Fig. 4g,h). The prey species varied at different depths. For instance, *Apolemia* sp. were mostly seen at 50–60 m, *Nanomia* sp. were observed 130–170 m, and *Praya* sp. were seen at 60–170 m (Fig. 4g).

The details of feeding events were characterized from the images taken every 4 s by MOLA7. Regarding feeding on scyphozoa, the sunfish approached a jellyfish and captured it, but the sunfish only fed on the gonads and oral arms of the jellyfish (Fig. 5a). A characteristic of this feeding event seen in the behavioural data was that the sunfish approached the jellyfish and decelerated (Fig. 5d). Regarding feeding on a siphonophore chain, the sunfish approached the chain and captured it, but the sunfish did not feed on the whole chain (possibly because the chain disassembled during feeding) (Fig. 5b). A characteristic of this feeding event was also that the sunfish approached the siphonophore chain with deceleration (Fig. 5e). However, there was another pattern of feeding on siphonophore chains where the sunfish approached the chain with acceleration (Fig. 5c,f).

Table 2. Information about prey items seen in the images recorded by the still camera

Fish ID	Interval (s)	Total no. of images	No. of images with prey items	Siphonophore			Scyphozoa	Ctenophore	Unknown
				Nanomia sp.	*Praya* sp.	*Apolemia* sp.			
MOLA1	30	15 517	81 (57)	55				1	1
MOLA3	30	12 837	14 (10)		9		1		
MOLA4	30	14 968	6 (6)	3	1		1	1	
MOLA7	4	4 354	222 (114)	65	5	37	3		4

The numbers in parentheses in the column of 'No. of images with prey items' show the numbers of images after removal of serial images that contain the same objects.

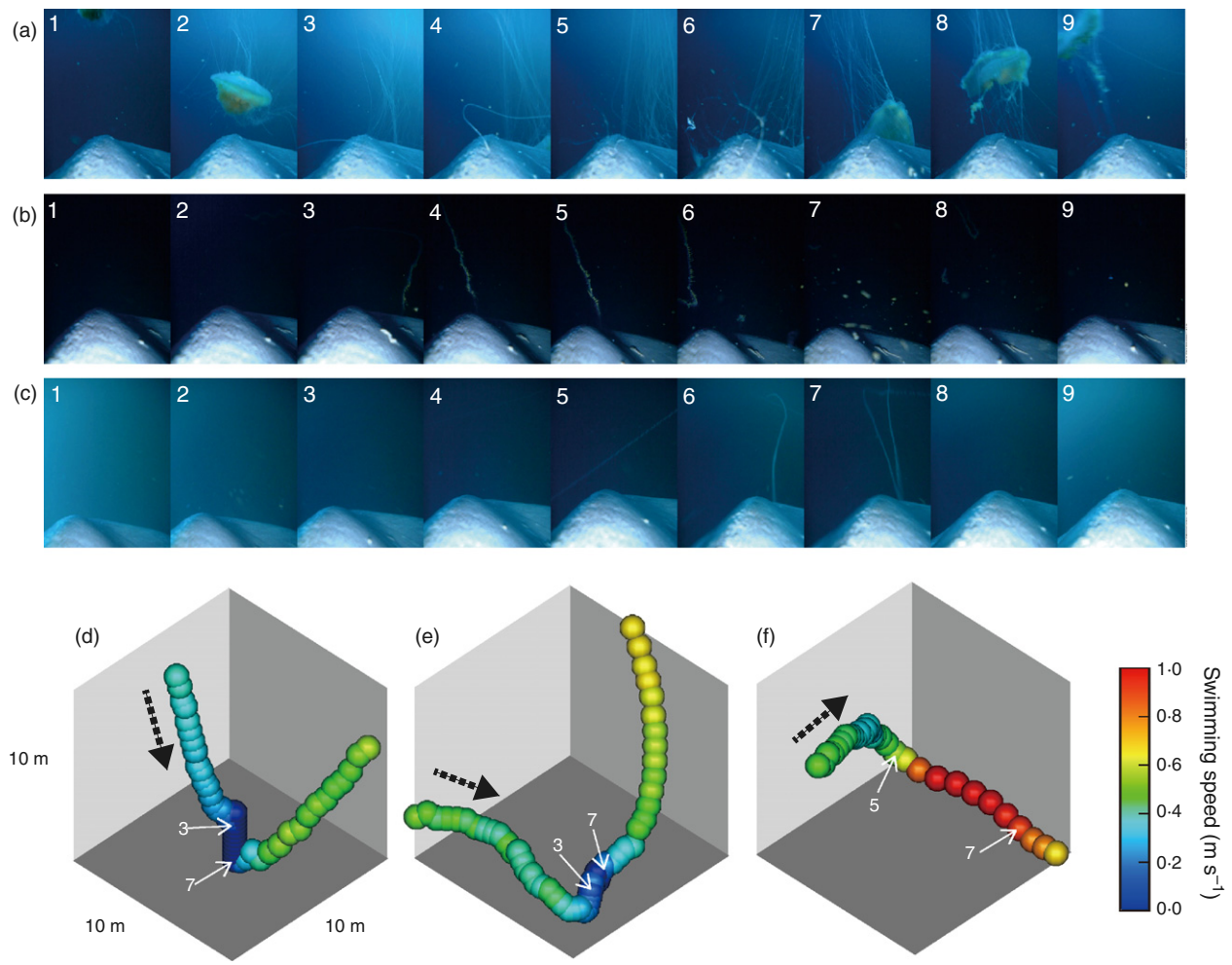

Fig. 5. Successive images taken at 4-s intervals (a–c) and 3D paths during feeding events (d–f). Colours of the 3D paths indicate swimming speed, and numbers with in the paths indicate the image numbers. (a, d) The sunfish approached a *Cyanea capillata* and stopped to feed. (b, e) The sunfish approached a *Praya* sp. and stopped to feed. (c, f) The sunfish rushed towards *Apolemia* sp. and fed.

Most of the feeding events were accompanied by deceleration or acceleration. Therefore, the swimming speed of the sunfish was used to detect each feeding event in the behavioural data. Feeding events with deceleration (decreased rate of swimming speed in 4 s that was greater than the standard deviation of the swimming speed) were defined as values below the mean swimming speed minus twice the standard deviation of swimming speed. Similarly, feeding events with acceleration (increased rate of swimming speed in 4 s that was greater than twice the standard deviation of swimming speed) were defined as values above the mean swimming speed plus twice the standard deviation of swimming speed. The mean and the standard deviation of swimming speed were calculated during the sunfish were active (swimming speed >0·2 m s^{-1}). These criteria were used to extract feeding events from the behavioural data recorded by all individuals (see an example, Fig. 6a,b).

Total feeding events with deceleration and acceleration were extracted 4794 times and 337 times, respectively, from the seven sunfish (Table 3). Seventy-eight per cent of the feeding events with acceleration occurred at shallower depths (<50 m) (Fig. 6c), while 75% of feeding events with deceleration occurred at 110–180 m (Fig. 6c). Ninety-five per cent of feeding events occurred during the day (Fig. 6d).

BODY TEMPERATURE

Before deep excursions, the body temperature of the sunfish was 16–20 °C, which was similar to the ambient water temperature at the surface, and it decreased to minimum 12 °C after deep excursions (Fig. 7a,b). After every deep excursion, the sunfish stayed at the surface, and their body temperatures rebounded to values similar to the sea surface temperature (Fig. 7a,b). Body temperature ranges of the sunfish (12–21 °C) were narrower than the range of ambient water temperature (3–22 °C) (Table 4). The mean body temperatures were 16–17 °C, and the mean ambient water temperatures were 14–16 °C (Table 4). The body temperature of the dead sunfish also changed with ambient water temperature (Fig. 7c).

Calculated BIC values became minimum at the response time-lag τ was 4–8 min, and were lower in the variable k model (*b*) than the constant k model (*a*) in all individuals in the field (Table 4, Fig. 8a–c). The estimated parameters for the BIC minimum model of each k condition are presented in Table 4. The values of k_1 and k_2 produced by the variable k model (*b*) generate warming and cooling curves, which match the observed body temperature changes (Fig. 7a,b). All individuals in the field showed lower heat-transfer coefficients during cooling (k_1) than during warming (k_2), and the rate of temperature change due to internal heat production ($\dot{T}_0$) was 0

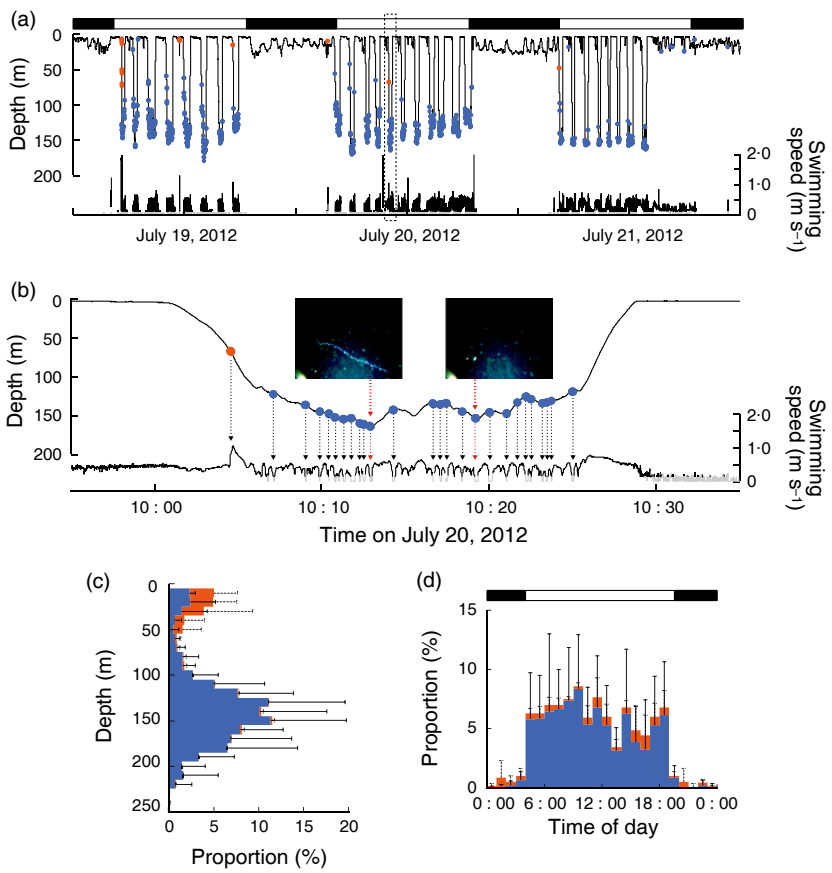

Fig. 6. (a) An example of the results of feeding event detection from MOLA1. Coloured dots indicate each feeding event with deceleration (blue) and acceleration (orange). The bar above the graph indicates night (black) and day (white). (b) Enlargement of a deep excursion (dotted box) in (a). Dotted arrows indicate the time each feeding event occurred, and red arrows indicate the true feeding events [prey items (*Nanomia* sp.) were seen in the images]. Swimming speed under the stall speed of the speed sensors (0·1–0·2 m s^{-1}) is shown in grey. (c, d) Frequency histograms of depth and time of day. Colours indicate the feeding events shown above. The histograms show the mean value of all individuals, and error bars represent standard deviations among individuals.

Table 3. Information regarding detected feeding events and deep excursions. Deep excursions were defined as the sunfish swam at depths >30 m for >4 min, and its duration was defined as time between the start of continuous descent (>2 min) before the deep excursion and the end of continuous ascent (>2 min) after the deep excursion. The deep excursions that occurred within 1 day after release were removed from analyses

Fish ID	Feeding events with deceleration	Feeding events with acceleration	No. of deep excursions	Duration of deep excursions (min) Mean ± SD	Maximum depth of deep excursions (m) Mean ± SD	Feeding events per deep excursion Mean ± SD
MOLA1	943	23	35	37·3 ± 9·2	163 ± 29	24·4 ± 12·8
MOLA2	279	38	53	41·5 ± 16·1	140 ± 26	33·6 ± 15·4
MOLA3	976	15	16	54·3 ± 27·8	199 ± 48	17·1 ± 17·8
MOLA4	108	22	12	41·3 ± 31·9	173 ± 89	8·7 ± 11·8
MOLA5	491	41	50	29·4 ± 8·4	139 ± 80	15·0 ± 10·0
MOLA6	1712	10	33	48·5 ± 17·0	159 ± 31	25·3 ± 15·2
MOLA7	302	185	18	29·8 ± 40·3	94 ± 75	16·4 ± 38·3

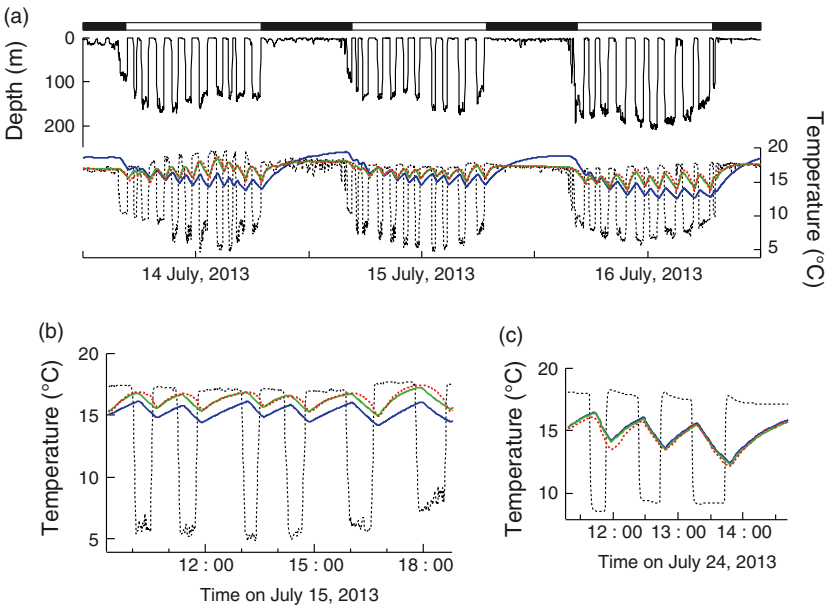

Fig. 7. Time-series depth, ambient temperature (dotted black line) and body temperature (coloured lines) of MOLA6 (a) and the enlarged data (b). The bar above the graph indicates night (black) and day (white). Body temperature colours indicate observed body temperature (dotted orange), and estimated body temperature using a model with a constant coefficient (blue) and variable coefficients (green). (c) Time series of ambient temperature and body temperature of the dead sunfish. Line colours are the same as above.

(Table 4). The estimated response time-lag τ was greater in larger individuals (Table 4). The ratios of k_1 and k_2 were similar among body sizes (Table 4), and both values of k_1 and k_2 decreased with sunfish body size (Fig. 8e). In case of the dead sunfish, model (*a*) showed lower BIC and body temperatures estimated by models (*a*) and (*b*) were similar to the observed body temperature (Table 4, Figs 7c and 8d). The heat-transfer coefficient of the dead sunfish was below the extension of the regression line of the heat-transfer coefficient of the living sunfish during cooling (Fig. 8e).

Discussion

FORAGING BEHAVIOUR

Historically, ocean sunfish were classified as slow, inactive animals, drifting passively with the currents. However, some tracking studies concluded they were active swimmers because of high travel speeds and movement against general current patterns (average rate of 10–20 km day^{-1}) (Cartamil & Lowe 2004; Sims *et al.* 2009a,b; Potter, Galuardi & Howell 2011). Dewar *et al.* (2010) revealed the seasonal migration pattern near Japan, which suggested their movement to higher latitudes as temperatures increased in the summer. However, in the present study, all of the ocean sunfish released in July moved south over 120 km away from the release point where the sea surface temperature was near 20 °C. The fish moved at high speeds during the migratory movement similar to other reports (>20 km day^{-1}) (Table 1). In the study area, the general ocean current in the coastal area is in a southward direction at 0·5–1 knots (≒22–44 km day^{-1}) (Japan Meteorological Agency 2013). The travel distance calculated by the dead-reckoning method covered <50% of the distance between the release and package pop-up locations (Table 1), suggesting that a major part of migration in ocean sunfish might depend on the ocean current. Recent satellite tracking suggested that ocean sunfish seek out thermal fronts where high productivity results in abundant prey (Dewar *et al.* 2010; Potter, Galuardi & Howell 2011). In the present study, primary productivity where

Table 4. Temperature information and result summary of parameter estimation using the heat-budget models

Fish ID	Total length (cm)	Ambient temperature (°C) Mean ± SD (min.–max.)	Body temperature (°C) Mean ± SD (min.–max.)	Models	k (°C min^{-1} °C^{-1})	k_1 (°C min^{-1} °C^{-1})	k_2 (°C min^{-1} °C^{-1})	$\dot{T}_0$ (°C min^{-1})	τ (min)	BIC	k_2/k_1
MOLA5	105	15·0 ± 3·2 (2·6–21·8)	16·1 ± 0·8 (12·0–18·2)	(*a*)	8·06 × 10^{-3}			8·63 × 10^{-3}	6	−42 508	
				(*b*)		6·23 × 10^{-3}	2·28 × 10^{-2}	0	5	−43 726	3·66
MOLA6	125	14·6 ± 3·9 (4·6–19·5)	16·4 ± 0·9 (13·4–18·6)	(*a*)	6·41 × 10^{-3}			1·20 × 10^{-2}	8	−35 298	
				(*b*)		4·33 × 10^{-3}	2·83 × 10^{-2}	0	7	−37 742	6·53
MOLA7	191	15·7 ± 3·4 (4·9–22·0)	16·9 ± 1·8 (13·3–20·7)	(*a*)	3·47 × 10^{-3}			4·57 × 10^{-3}	7	−41 632	
				(*b*)		2·17 × 10^{-3}	8·75 × 10^{-3}	0	7	−42 689	4·03
Dead	32			(*a*)	2·30 × 10^{-2}			0	4	−1022	
				(*b*)		2·36 × 10^{-2}	2·15 × 10^{-2}	0	3	−1020	0·91

BIC, Bayesian information criterion.

sunfish moved was not higher than the other area around study site (Fig. 2). However, there is less information about the horizontal distribution of ocean sunfish prey. The area where sunfish moved to in the present study may be a good foraging ground because all individuals exhibited frequent feeding events.

Ocean sunfish were diurnally active, while inactive in a lateral position during the night. Ocean sunfish achieve a slightly negative buoyancy without swim bladder (Watanabe & Sato 2008), and the lateral position during the night might help the fish avoid sinking because the body is laterally flattened. During the day, the sunfish repeated surfacing and periodic deep excursions. These deep excursions were thought to relate to foraging, but there has been no supporting empirical evidence (Hays *et al*. 2009; Sims *et al*. 2009a; Potter & Howell 2011). In the present study, visual evidence that ocean sunfish fed on gelatinous zooplanktons in deep water was first obtained. The prey items included various gelatinous zooplanktons, such as a large scyphozoa, ctenophores and various siphonophore chains (at least three species). The serial images also revealed that ocean sunfish only fed on parts of jellyfish such as gonads and oral arms and left the bell intact. The gonads and oral arms of jellyfish contain higher energy than the bell (Doyle *et al*. 2007). Therefore, ocean sunfish may only feed on energy-rich parts of these jellyfishes. The species of siphonophores in the images varied based on depth and one individual (MOLA7) fed on different species of siphonophores at different depths on the same day. Ocean sunfish might change the maximum depth of deep excursions to consume a wide range of siphonophore species that are distributed at different depths.

The depth distribution of the detected feeding events using swimming speed was consistent with the peak occurrence of siphonophores in the still images. Siphonophores are known to exhibit diel vertical migration, that during the day they remain at deep depths and travel to shallow waters at night (Silguero & Robison 2000). Furthermore, studies using satellite tracking suggested that ocean sunfish occupy significantly greater depths during the day. This behaviour matches the strategy of normal diel vertical migration and has been attributed to a strategy of near continual feeding on vertically migrating prey (Hays *et al*. 2009; Sims *et al*. 2009a). However, few prey items (no siphonophores) were seen in the images recorded during the night. The ocean sunfish in the present study were clearly diurnal in that they foraged only during the day and were almost inactive during the night, thus indicating that their diel pattern might not be related to a continual feeding strategy.

There were two different types of foraging events: one was accompanied with deceleration and the other was accompanied with acceleration. The former behaviour is consistent with foraging on slow moving prey (Narazaki *et al*. 2013), but the sunfish also accelerated to catch such slow moving prey. The feeding events with deceleration occurred mostly in deep water during the day, while the feeding events with acceleration were more common in

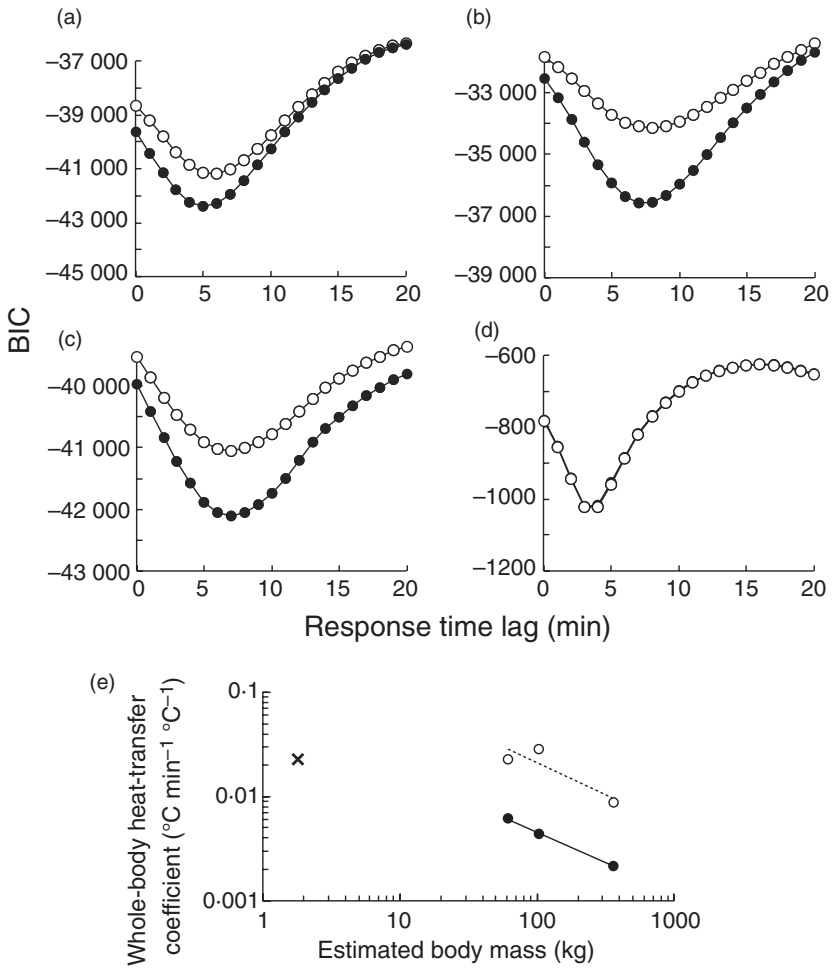

Fig. 8. Relationship between the response time-lag τ and the Bayesian information criterion (BIC) of models using a constant coefficient (open circles) and variable coefficients (black circles) for (a) MOLA5, (b) MOLA6, (c) MOLA7 and (d) a dead individual. (e) Relationship between the estimated body masses and estimated heat-transfer coefficients. Circles show the sunfish in the field of the heat-transfer coefficients during cooling (black) and during warming (open), and a cross mark indicates the heat-transfer coefficient of the dead individual, which was constant during both cooling and warming.

shallower water. In the still images taken in shallow water, silhouettes of the prey objects were recognized from a distance. Diurnal foraging and feeding with acceleration in shallow water suggest that ocean sunfish might visually search for prey. Some siphonophores use bioluminescence for bait attraction (Haddock & Case 1999; Haddock *et al.* 2005), and this may also enable ocean sunfish to find prey in deep water. The visual acuity of ocean sunfish, calculated from peak ganglion cell densities, was 3·51–4·33 cycles per degree, which is comparable to adult sharks (2·8–3·7 cycles per degree) (Kino *et al.* 2009). Therefore, sunfish may possibly prefer diurnal foraging because they may need light to visually find their prey; however, other studies have shown that sunfish are active during both day and night to depths >50 m (Sims *et al.* 2009a), which suggests that they might rely on bioluminescent prey.

THERMOREGULATION

Behavioural thermoregulation using vertical temperature environment is observed in both endothermic and ectothermic marine species (Carey & Scharold 1990; Holland & Sibert 1994; Kitagawa *et al.* 2001; Casey, James & Williard 2014). The hypothesis of thermal recovery is one of the most widely cited to explain the vertical oscillating of various pelagic fishes (e.g. Compana *et al.* 2011; Thums *et al.* 2012). Previous tracking studies suggested that the surfacing behaviour of ocean sunfish also might be related to behavioural thermoregulation (Cartamil & Lowe 2004; Sims *et al.* 2009a; Dewar *et al.* 2010; Potter & Howell 2011), but no evidence was indicated. Cartamil & Lowe (2004) demonstrated that a significant relationship exists between the maximum dive depth and the ensuing post-dive surface period. In the present study, the body temperatures of the sunfish were first recorded. Oceanic water around the study site was highly stratified with a narrow surface mixed layer, and the ambient water temperature decreased with depth. Therefore, the body temperature of the sunfish decreased during foraging in deep, cold water, but rebounded during subsequent surfacing period. This indicates that a function of surfacing is behavioural thermoregulation to recover body temperature in warm surface water.

The results of the catch survey suggest that ocean sunfish were mostly caught at 15–17 °C (Nakamura & Sato 2014), and this is similar to the mean body temperature in this study (16–17 °C). However, the prey of ocean sunfish is distributed in colder water (5–12 °C). The analyses using heat-budget models indicated that whole-body heat-transfer coefficients during warming were larger than that

during cooling, suggesting that ocean sunfish might be able to change heat exchange between the surrounding water. The estimated heat-transfer coefficients also indicated that smaller individuals had larger coefficients. In addition, the dead individual showed constant heat-transfer coefficient, which was close to the regression line of the heat-transfer coefficients during cooling of living sunfish. These results indicate that ocean sunfish may efficiently gain heat from the warm surface water by physiological regulation. Accordingly, the mean body temperature of ocean sunfish was 1–2 °C warmer than mean ambient water temperature. Similar body temperature changes were observed in other ectothermic fishes. For instance, in blue sharks (*P. glauca*), the cooling rate was smaller than the warming rate, which enabled them to maintain a mean body temperature that was 4 °C warmer than the mean ambient water temperature (Carey & Scharold 1990). These gaps between body and ambient water temperature were smaller than those of endothermic species, such as porbeagles, mako sharks and bluefin tunas, which produce internal heat and effectively reduce heat loss using counter current heat exchange systems (Carey & Teal 1969a,b). In the present study, internal heat production was not necessary to explain body temperature change of ocean sunfish, suggesting they do not have thermogenic activity. A passive thermoregulatory strategy, which depends on the physical attributes of their large body masses rather than physiological mechanisms, was described in adult loggerhead sea turtles (Sato 2014). The larger sunfish had lower heat-transfer coefficients, suggesting they also benefit from their large body masses to keep their body warm in cold water.

However, the physiological mechanisms required to efficiently gain heat are still in question. One possibility is that fish can alter blood flow between cooling and warming, which has been described in sea turtles (Hochscheid, Bentivegna & Speakman 2002). Fish gills have 2–48 times greater surface area than body surface area (Gray 1954), and this larger surface area of the gills might work as a heat exchanger. Ocean sunfish may increase blood flow through their gills to increase heat exchange at their gills while in the warmer surface waters.

CYCLES OF VERTICAL MOVEMENTS IN RELATION TO FORAGING UNDER TEMPERATURE CONSTRAINT

To maximize fitness, animals acquire resources with the lowest energy expenditure (Pyke 1984). To increase amount of food intake, there are two strategies: the first is increase foraging efficiency per unit time, and the second is increase time to devote to foraging. In the present study, cycles of deep foraging and surface warming might be related to optimal foraging behaviour of ocean sunfish. Therefore,

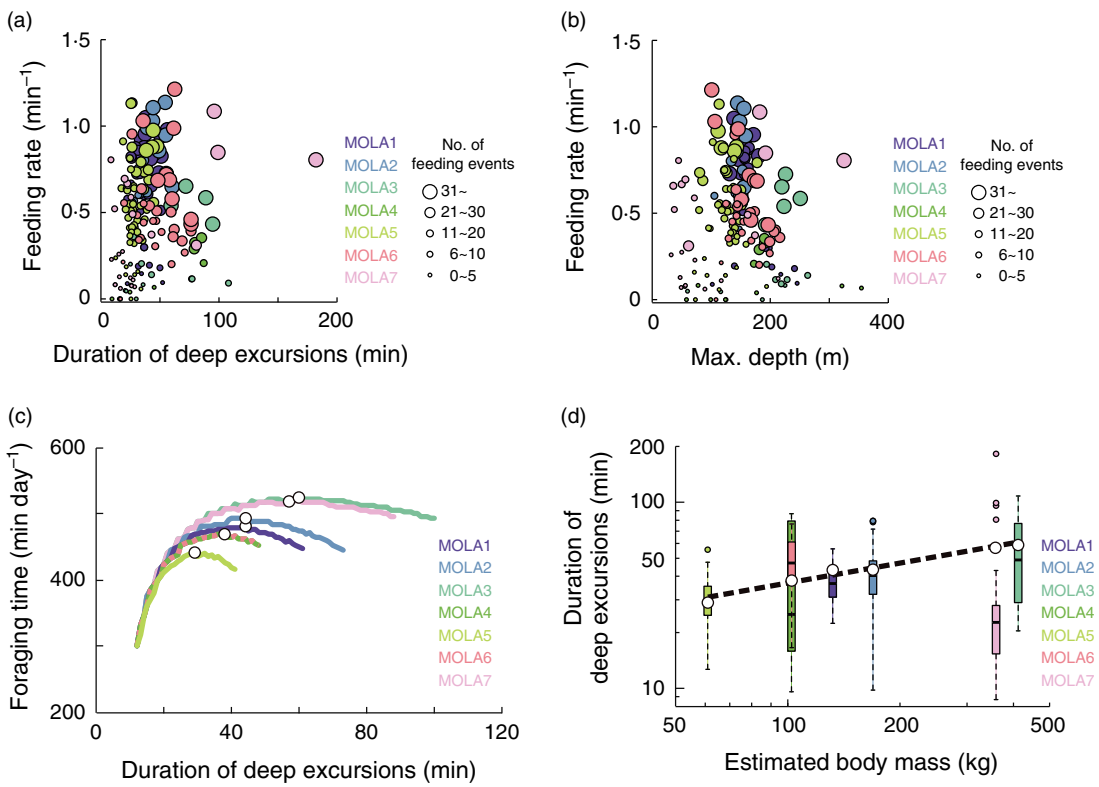

Fig. 9. Relationships between feeding rate (feeding events per minute) during a deep excursion and (a) duration or (b) maximum depth of the deep excursion. Colours of the circles indicate individuals, and circle sizes indicate the number of feeding events. (c) Estimated curves of foraging time against durations of deep excursions. White circles show the duration when foraging time peaks. (d) Boxplots of observed duration of deep excursions against body mass. White circles also show efficient durations and a dotted line shows power approximation for these.

what determines cycles of vertical movements were examined in terms of foraging and thermoregulation.

To test whether feeding efficiency were different among durations or depths of deep excursion, feeding rate (extracted feeding events per minute) during each deep excursion was compared to duration or maximum depth of the deep excursion (Table 3). Generalized linear mixed models and Akaike information criteria (AIC) were used to select the most parsimonious model. The 'glmer' function with a gamma error contained in the 'lme4' package in R ver. 3.0.2 (R Core Team 2013) was used to calculate AIC. Feeding rate was set as response variables in the models, duration and maximum depth were set as explanatory variables, and individuals were set as a random effect. A null model, which did not include duration and maximum depth, showed the lowest AIC (AIC = 97·0, 1·6 smaller than AIC of the models including duration or maximum depth), indicating that feeding rate (foraging efficiency) was not related to duration and maximum depth of deep excursions (Fig. 9a,b). This suggests that increasing foraging time is effective for increasing total amount of food intake.

Then, to test whether cycles of vertical movements were different among body size, the duration of deep excursions, which maximized foraging time, was estimated using the parameters estimated by the heat-budget models. Each cycle consists of a deep excursion for foraging and subsequent surfacing for rewarming, and a deep excursion includes travelling between the surface and deep water. To obtain time required for each cycle, time required for recovering body temperature, which decreased during a deep excursion, was estimated. We assumed 15 °C as the minimum of body temperature because all three individuals with body temperature showed similar means of the minimum body temperatures after deep excursions (14·8–14·9 °C). Heat-transfer coefficients during cooling and warming were estimated from the relationships between coefficients and body mass (Fig. 8e). The modes of water temperature during deep excursions and surfacing were 10 and 17 °C, respectively (Fig. 3c). Therefore, we set 10 and 17 °C as ambient water temperature during cooling and warming, respectively. We used 8 min as round-trip time for travelling between the surface and deep water. The daytime (1000 min) was divided by time required for a cycle and obtained the number of cycles, then computed total foraging time by multiplying foraging time in a cycle and the number of cycles. Total foraging time against durations of deep excursions showed concave down curves, and the duration when total foraging time peaked was assumed as an efficient duration to maximize foraging time (Fig. 9c). The efficient duration became longer in larger individuals and included within ranges of observed durations of deep excursions in all individuals except MOLA7 (Fig. 9d). Staying in cold water longer, time required for rewarming becomes longer, and time ratio of deep excursions to surfacing becomes smaller (Fig. 10). This indicates frequent back and forth between the surface and deep water can reduce time required for rewarming; however, frequent back and forth requires more travelling time and decreases foraging time (Fig. 10). Thus, there is an efficient duration of deep excursion, and estimated efficient durations were longer in larger individuals because cooling speed was

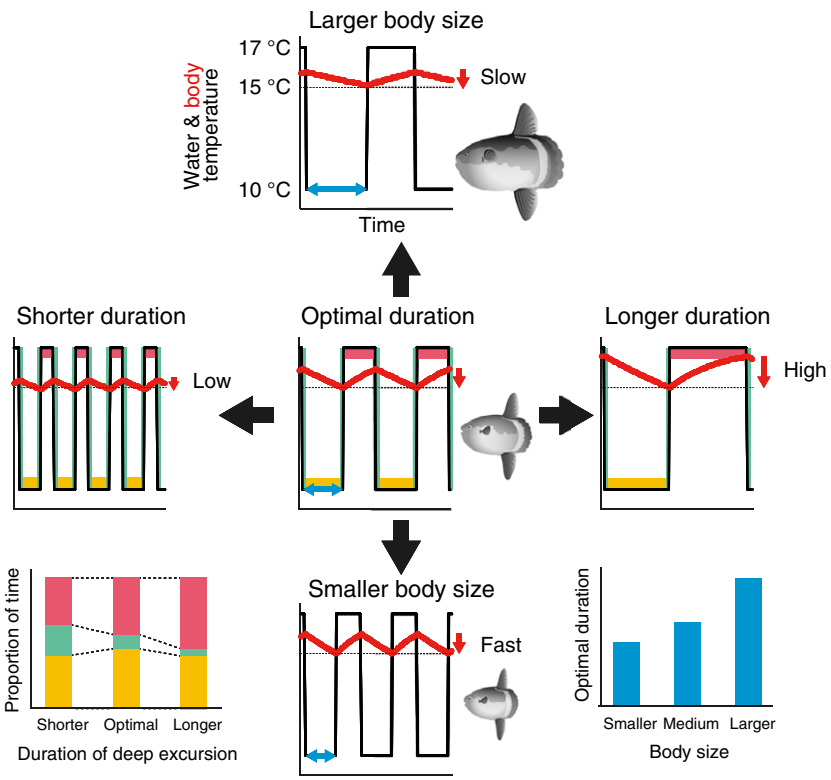

Fig. 10. Schematic diagram of cycles of deep excursions in relation to duration of deep excursions in the same size (transversally arranged) and optimal cycles in relation to body sizes (longitudinally arranged). Black and red lines show ambient water temperature and estimated body temperature, respectively. Red arrows on the right of temperatures indicate magnitudes of body temperature changes. Colours of the bars indicate foraging (yellow), travelling (green) and surfacing (red), and blue arrows indicate optimal duration in each body size. There is an optimal duration of deep excursions to increase foraging time, and an optimal duration is longer in larger individuals.

slower when body size becomes larger (Fig. 10). Observed durations of deep excursions of all individuals except MOLA7 were consistent with the estimated efficient duration. The maximum depths of deep excursions of MOLA7 were shallower than that of other individuals (Table 3). Time required for travelling between the surface and deep water becomes shorter in case of shallower excursions, and if travelling time becomes shorter, efficient duration of excursions also becomes shorter. This might be why MOLA7 showed shorter durations of deep excursions. These suggest that durations of deep excursions of ocean sunfish are not related to feeding rate but are associated with maximizing their foraging time in cycles of vertical movements.

CONCLUSIONS

In the present study, the evidences of foraging siphonophores in deep water and behavioural thermoregulation of ocean sunfish were empirically demonstrated. From a morphological aspect, ocean sunfish have a rounded and flattened large body and thick skin, and lack a swim bladder (Watanabe & Sato 2008). These characteristics might have advantages of foraging for deep-sea organisms; for example, buoyancy control without a swim bladder enables them to make frequent back and forth between the surface and deep water, their thick skin and large body might reduce heat loss in deep, cold water, and flattened body might enhance floating at the surface to rewarm after deep foraging. Ocean sunfish seem to benefit from their large body masses, which increase total foraging time in an environment with vertical temperature gradient. These adaptations to pelagic habitat and abundant food source in deep-sea ecosystems might enable ocean sunfish to become the world heaviest teleost.

Acknowledgements

This study was supported by Bio-Logging Science at the University of Tokyo (UTBLS), the Grants-in-Aid for Scientific Research from the Japan Society of the Promotion of Science (12J07184, 25660152, 24241001), the Canon Foundation, Project Grand Maillet and the Cooperative Program of Atmosphere and Ocean Research Institute at the University of Tokyo. We thank Dr. Dhugal J. Lindsey for the identification of jellyfish species. We thank Dr. Thomas Doyle for his valuable suggestions to improve the quality of the paper. We deeply thank chief Hideo Sasaki and the fishermen of the Funakoshi Bay Fisheries Cooperative, and captain Hiroshi Shozushima and the crew of the 'Koyo-maru' boat.

Data accessibility

Data available from the Dryad Digital Repository: http://dx.doi.org/10.5061/dryad.84393 (Nakamura, Goto & Sato 2015).

References

Abe, T., Sekiguchi, K., Onishi, H., Muramatsu, K. & Kamito, T. (2012) Observations on a school of ocean sunfish and evidence for a symbiotic cleaning association with albatrosses. *Marine Biology*, **159**, 1173–1176.

Angel, M.V. & Baker, A.D.C. (1982) Vertical distribution of the standing crop of plankton and micronekton at three stations in the Northeast Atlantic. *Biological Oceanography*, **2**, 37–41.

Aoki, K., Amano, M., Mori, K., Kourogi, A., Kubodera, T. & Miyazaki, N. (2012) Active hunting by deep-diving sperm whales: 3D dive profiles and maneuvers during bursts of speed. *Marine Ecology Progress Series*, **444**, 289–301.

Brunnschweiler, J.M., Baensch, H., Pierce, S.J. & Sims, D.W. (2009) Deep-diving behaviour of a whale shark *Rhincodon typus* during long-distance movement in the western Indian Ocean. *Journal of Fish Biology*, **74**, 706–714.

Carey, F.G. & Robison, B.H. (1981) Daily patterns in the activities of swordfish, *Xiphias gladius*, observed by acoustic telemetry. *Fishery Bulletin*, **79**, 277–292.

Carey, F.G. & Scharold, J.V. (1990) Movements of blue sharks (*Prionace glauca*) in depth and course. *Marine Biology*, **342**, 329–342.

Carey, F.G. & Teal, J.M. (1969a) Mako and porbeagle: warm-bodied sharks. *Comparative Biochemistry and Physiology*, **28**, 199–204.

Carey, F.G. & Teal, J.M. (1969b) Regulation of body temperature by the bluefin tuna. *Comparative Biochemistry and Physiology*, **28**, 205–213.

Cartamil, D.P. & Lowe, C.G. (2004) Diel movement patterns of ocean sunfish *Mola mola* off southern California. *Marine Ecology Progress Series*, **266**, 245–253.

3Casey, J.P., James, M.C. & Williard, A.S. (2014) Behavioral and metabolic contributions to thermoregulation in freely swimming leatherback turtles at high latitudes. *Journal of Experimental Biology*, **217**, 2331–2337.

Compana, S.E., Dorey, A., Fowler, M., Joyce, W., Wang, Z., Wright, D. *et al.* (2011) Migration pathways, behavioural thermoregulation and overwintering grounds of blue sharks in the Northwest Atlantic. *PLoS ONE*, **6**, e16854.

Dewar, H., Thys, T., Teo, S.L.H., Farwell, C., O'Sullivan, J., Tobayama, T. *et al.* (2010) Satellite tracking the world's largest jelly predator, the ocean sunfish, *Mola mola*, in the Western Pacific. *Journal of Experimental Marine Biology and Ecology*, **393**, 32–42.

Doyle, T.K., Houghton, J.D.R., McDevitt, R., Davenport, J. & Hays, G.C. (2007) The energy density of jellyfish: estimates from bomb-calorimetry and proximate-composition. *Journal of Experimental Marine Biology and Ecology*, **343**, 239–252.

Gray, I.E. (1954) Comparative study of the gill area of marine fishes. *Biological Bulletin*, **107**, 219–225.

Haddock, S.H.D. & Case, J.F. (1999) Bioluminescence spectra of shallow and deep-sea gelatinous zooplankton: ctenophores, medusae and siphonophores. *Marine Biology*, **133**, 571–582.

Haddock, S.H.D., Dunn, C.W., Pugh, P.R. & Schnitzler, C.E. (2005) Bioluminescent and red-fluorescent lures in a deep-sea siphonophore. *Science*, **309**, 263.

Hays, G.C., Farquhar, M.R., Luschi, P., Teo, S.L.H. & Thys, T.M. (2009) Vertical niche overlap by two ocean giants with similar diets: ocean sunfish and leatherback turtles. *Journal of Experimental Marine Biology and Ecology*, **370**, 134–143.

Hochscheid, S., Bentivegna, F. & Speakman, J.R. (2002) Regional blood flow in sea turtles: implications for heat exchange in an aquatic ectotherm. *Physiological and Biochemical Zoology*, **75**, 66–76.

Holland, K.N. & Sibert, J.R. (1994) Physiological thermoregulation in bigeye tuna, *Thunnus obesus*. *Environmental Biology of Fishes*, **40**, 319–327.

Houghton, J.D.R., Liebsch, N., Doyle, T.K., Gleiss, A.C., Lilley, M.K.S., Wilson, R.P. *et al.* (2009) Harnessing the sun: testing a novel attachment method to record fine scale movements in ocean sunfish (*Mola mola*). *Tagging and Tracking of Marine Animals with Electronic Devices, Reviews: Methods and Technologies in Fish Biology and Fisheries*, **9**, 229–242.

Japan Meteorological Agency (2013) Japan Meteorological Agency Website. http://www.data.jma.go.jp/gmd/kaiyou/shindan/index.html.

Kino, M., Miayzaki, T., Iwami, T. & Kohbara, J. (2009) Retinal topography of ganglion cells in immature ocean sunfish, *Mola mola*. *Environmental Biology of Fishes*, **85**, 33–38.

Kitagawa, T., Nakata, H., Kimura, S. & Tsuji, S. (2001) Thermoconservation mechanisms inferred from peritoneal cavity temperature in free-swimming Pacific bluefin tuna *Thunnus thynnus orientalis*. *Marine Ecology Progress Series*, **220**, 253–263.

Kloeden, P.E. & Platen, E. (1999) *Numerical Solution of Stochastic Differential Equations*, 3rd edn. Springer, Berlin.

Naito, Y., Costa, D.P., Adachi, T., Robinson, P.W., Fowler, M. & Takahashi, A. (2013) Unravelling the mysteries of a mesopelagic diet: a large

apex predator specializes on small prey. *Functional Ecology*, **27**, 710–717.

Nakamura, I., Goto, Y. & Sato, K. (2015) Data from: Ocean sunfish rewarm at the surface after deep excursions to forage for siphonophores. *Dryad Digital Repository*, http://dx.doi.org/10.5061/dryad.84393

Nakamura, I. & Sato, K. (2014) Ontogenetic shift in foraging habit of ocean sunfish *Mola mola* from dietary and behavioral studies. *Marine Biology*, **161**, 1263–1273.

Narazaki, T., Sato, K., Abernathy, K.J., Marshall, G.J. & Miyazaki, N. (2013) Loggerhead tuetles (*Caretta caretta*) use vision to forage on gelatinous prey in mid-water. *PLoS ONE*, **8**, e66043.

Pope, E.C., Hays, G.C., Thys, T.M., Doyle, T.K., Sims, D.W., Queiroz, N. *et al*. (2010) The biology and ecology of the ocean sunfish *Mola mola*: a review of current knowledge and future research perspectives. *Reviews in Fish Biology and Fisheries*, **20**, 471–487.

Potter, I.F., Galuardi, B. & Howell, W.H. (2011) Horizontal movement of ocean sunfish, *Mola mola*, in the northwest Atlantic. *Marine Biology*, **158**, 531–540.

Potter, I.F. & Howell, W.H. (2011) Vertical movement and behavior of the ocean sunfish, *Mola mola*, in the northwest Atlantic. *Journal of Experimental Marine Biology and Ecology*, **396**, 138–146.

Pyke, G.H. (1984) Optimal foraging theory: a critical review. *Annual Review of Ecology and Systematics*, **15**, 523–575.

Queiroz, N., Humphries, N.E., Noble, L.R., Santos, A.M. & Sims, D.W. (2012) Spatial dynamics and expanded vertical niche of blue sharks in oceanographic fronts reveal habitat targets for conservation. *PLoS ONE*, **7**, e32374.

R Core Team (2013) *R: A Language and Environment for Statistical Computing*. R Foundation for Statistical Computing, Vienna, Austria. http://www.R-project.org/.

Sato, K. (2014) Body temperature stability achieved by the large body mass of sea turtles. *Journal of Experimental Biology*, **217**, 3607–3614.

SEATURTLE.ORG Maptool (2002) SEATURTLE.ORG, Inc. http://www.seaturtle.org/maptool/.

Shiomi, K., Narazaki, T., Sato, K., Shimatani, K., Arai, N., Ponganis, P. *et al*. (2010) Data-processing artefacts in three-dimensional dive path reconstruction from geomagnetic and acceleration data. *Aquatic Biology*, **8**, 289–294.

Silguero, J.M.B. & Robison, B.H. (2000) Seasonal abundance and vertical distribution of mesopelagic calycophoran siphonophores in Monterey Bay, CA. *Journal of Plankton Research*, **22**, 1139–1153.

Sims, D.W., Queiroz, N., Doyle, T.K., Houghton, J.D.R. & Hays, G.C. (2009a) Satellite tracking of the World's largest bony fish, the ocean sunfish (*Mola mola* L.) in the North East Atlantic. *Journal of Experimental Marine Biology and Ecology*, **370**, 127–133.

Sims, D.W., Queiroz, N., Humphries, N.E., Lima, F.P. & Hays, G.C. (2009b) Long-term GPS tracking of ocean sunfish *Mola mola* offers a new direction in fish monitoring. *PLoS ONE*, **4**, e7351.

Thorrold, S.R., Afonso, P., Fontes, J., Braun, C.D., Santos, R.S., Skomal, G.B. *et al*. (2014) Extreme diving behaviour in devil rays links surface waters and the deep ocean. *Nature Communications*, **5**, 4274.

Thums, M., Meekan, M., Stevens, J., Wilson, S. & Polovina, J. (2012) Evidence for behavioural thermoregulation by the world's largest fish. *Journal of the Royal Society Interface*, **10**, 20120477.

Watanabe, Y. & Sato, K. (2008) Functional dorsoventral symmetry in relation to lift-based swimming in the ocean sunfish *Mola mola*. *PLoS ONE*, **3**, e3446.

Received 13 October 2014; accepted 22 January 2015
Handling Editor: Graeme Hays